

CALORIMETRIC CHARACTERIZATION OF 2',3'-DIDEOXYINOSINE WATER SOLUTION

Stability and interaction with human serum albumin

Katarzyna Michalik*, Zofia Drzazga and Anna Michnik

University of Silesia, A. Chelkowski' Institute of Physics, Department of Medical Physics, ul. Uniwersytecka 4, 40-007 Katowice, Poland

A study of 2',3'-dideoxyinosine (ddI) stability and its interaction with human serum albumin (HSA) was carried out by differential scanning microcalorimetry DSC. Scan rate dependent and irreversible endothermic thermal degradation of ddI was analyzed with use of kinetic approach. Observed process could be interpreted in terms of simple first-order one step kinetic model. Moreover it was shown that ddI bound weakly to the human serum albumin and stabilized this protein.

Keywords: 2',3'-dideoxyinosine, differential scanning microcalorimetry, human serum albumin, kinetic

Introduction

Human immunodeficiency virus (HIV) and acquired immune deficiency syndrome (AIDS) has become a major contributor to global morbidity and mortality. At the end of 2006, 39.5 million people worldwide were estimated to be living with HIV infection [1]. Patients infected with HIV have to be polymedicated for the rest of their lives. This fact explains the constant search, not only for new and more powerful drugs, but also for more effective formulation of already known drugs. The knowledge about decomposition reactions of drugs at various temperatures is important for prediction of storage conditions for drug formulation and behavior in human organism considered as water environment.

Antiretroviral drugs show ability to plasma proteins binding. But only the unbound fraction of drugs in plasma can reach the chronically infected cellular reservoir of HIV and pass across cell membranes to gain cross to viral enzymes located intracellularly in infected cells [2].

2',3'-dideoxyinosine (ddI) is a nucleoside analog reverse transcriptase inhibitor (NRT) used in AIDS treatment to suppress HIV replication. It is a dideoxy analogue of the purine nucleoside inosine that potently inhibits the replication of human immunodeficiency virus HIV. The ddI requires intercellular metabolism to the active triphosphate, 2',3'-dideoxyadenosine-5'-triphosphate (ddATP), which acts as competitive inhibitor of HIV reverse transcriptase or as a DNA chain terminator [3]. 2',3'-dideoxyinosine is white crystalline powder with molecular formula $C_{10}H_{12}N_4O_3$ and molecular mass

236.2. It is unstable in acid solutions. At $pH < 3$ ddI decomposes to hypoxanthine in less than 2 min.

The calorimetric method could be helpful in intermolecular (interaction with molecules) or intramolecular (substance stability) recognition, lately under molecular crowding conditions also [4]. Understanding the relationship between the structure of molecules and the energetic of their stability and binding with others molecules is indispensable in drug design [5–7]. An important consideration in drug design is the optimization of the binding affinity against the desired target with simultaneous minimizing the affinity of drug for unwanted targets. On the list on unwanted targets are the serum proteins: human serum albumin (HSA) and alpha1-cid glycoprotein (AAG), which are known to bind organic molecules in non-specific ways. These proteins exist in relatively high concentrations, and therefore, have the potential to significantly lower effective drug concentrations to suboptimal levels even if their affinity for drug molecules is not very high. The specific binding of drugs to serum proteins is important not only from the point of view of bioavailability, but also from the point of development of drug resistance. Antiretroviral therapy at suboptimal plasma levels does not eliminate completely viral replication, thereby contributing to the appearance of drug resistant viral strains [8].

The aim of the present study was to examine the stability of ddI aqueous solution and its interaction with human serum albumin. Differential scanning microcalorimetry (DSC) and UV V is spectrophotometry were used as a main and assistant measurement method, respectively.

* Author for correspondence: kasia_michalik1@wp.pl

Experimental

Materials

ddI was purchased from Bristol Myers Squibb, HSA was purchased from Sigma Chemical Co. (Sigma Lot 111K7612).

Aqua pro injection was used as a solvent in all experiments.

Preparation of samples

An accurately weighed amount of ddI was dissolved in aqua pro injection or in HSA aqueous solution (0.0155 mM). ddI solutions were prepared with the concentration from the range 1.5 to 6.2 mM. pH of the solution was 5.5 ± 0.4 .

Methods

DSC scans were performed using the VP DSC ultrasensitive microcalorimeter (MicroCal Inc., Northampton, MA) with cell volumes of 0.5 mL. Heat capacity *vs.* temperature profiles were obtained for scanning rates of 0.3, 0.5, 0.6, 1.0 and 1.5 K min⁻¹ in temperature range 25–130°C. Additionally constant pressure of about 1.8 atm over the liquids in the cells was applied. Samples were degassed immediately before loading the cells.

For concentration determination UV V is spectra of the samples were recorded in the wavelength range of 190–300 nm on JASCO V-530 spectrophotometer with 2 nm band-width and using 1.0 cm path length quartz cuvettes. In all experiments concentration of the sample was corrected with use of the calculated extinction coefficient 10683 ± 85 mol dm⁻³ at 249 nm.

Statistical analysis

The calorimetric data were corrected for the instrumental baseline water–water. A linear baseline was used to obtain the excess apparent molar heat capacity (C_p^{ex}). DSC curves were analyzed with MicroCal Origin software. The fit of the curves of the theoretical model to the experimental data was achieved by the non-linear Levenberg–Marquadt method.

Statistical analysis of the results was done with Statistica 7.1 using ANOVA. Schapiro–Wilk and Levene tests were performed to check the normality of the distributions and homogeneity of variance, respectively.

Results and discussion

Characteristic of ddI thermal transition

Figure 1 shows an original DSC excess molar heat capacity (C_p^{ex}) profiles for thermal degradation of ddI in water solution for different scanning rates (after subtracted water–water scan and concentration normalization).

The main endothermic transition is probably connected with degradation of ddI molecule to hypoxanthine [2]. For the highest scan rate ($v=1.5$ K min⁻¹) additional broad minimum in temperature range 45–90°C is present. Moreover the unformed endotherm around 40°C and inception of high temperature peaks can be seen for 0.3 and 1.5 K min⁻¹ but not for the other heating rates. These endotherms are hardly distinguishable from the measurement uncertainties but their enhancement is not possible due to the poor solubility of ddI, therefore they were not taken into further analysis.

The main ddI endotherms are shifted toward higher temperatures with scan rate increasing. The temperature T_m corresponding to the maximum heat capacity (C_p^m), change from 102.1 ± 0.3 to 115.2 ± 1.0 °C with scan rate rising from 0.3 to 1.5 K min⁻¹. It implies that the thermal degradation process of ddI water solution is kinetically determined.

The reversibility of the process was checked by reheating the drug solution in calorimetric cell after the cooling from the first run. No transition was obtained in the second run of all the samples (not shown).

The effect of the drug concentration on the position of the T_m gives some information about the changes in molecularity occurring during the thermal process. One can see from Table 1 the enthalpy change ΔH_{cal} (determined as the area framed by the heat capacity peak and transition baseline), T_m and

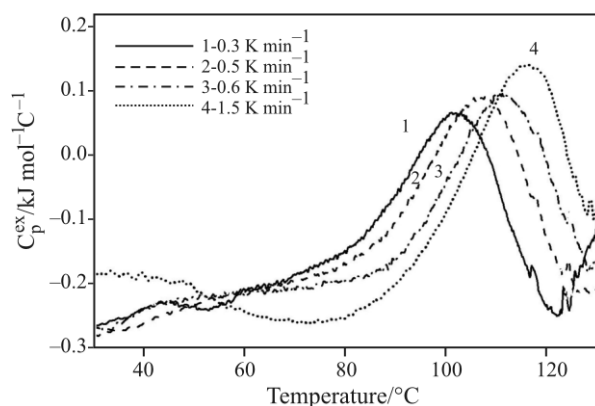


Fig. 1 Scan rate dependence of DSC ddI curves (concentration 3.1 mM)

Table 1 Thermodynamic parameters obtained from DSC scan of ddi at different drug concentrations L

L / mM	$\Delta H_{cal}/$ $\text{kJ mol}^{-1} \text{ } ^\circ\text{C}^{-1}$	$T_m/$ $^\circ\text{C}$	HHW/ $^\circ\text{C}$
1.5	5.7 ± 1.3	104.3 ± 1.7	18.8 ± 2.1
3.1	6.2 ± 2.5	102.1 ± 0.3	19.3 ± 1.8
4.7	5.8 ± 0.9	102.3 ± 0.8	20.4 ± 1.5
6.2	7.5 ± 1.5	102.0 ± 1.0	20.5 ± 2.5

half height width (HHW) are practically constant within error range.

Figure 2 presents DSC curves for fresh sample, after 6 and 12 h

Comparing analysis were done only for fresh samples because 6 h later T_m shift toward lower temperatures was observed again.

Interaction of ddi with HSA

The effect of ddi concentration on DSC transition of HSA at the heating rate 1.0 K min^{-1} is presented in Fig. 3.

The HSA–ddi curves are characterized by a single denaturation peak in temperature range from 60 to 90°C . It should be noted that small maximum on left DSC curve branch of HSA disappeared in ddi presence. Endotherms shifts toward higher temperatures and become more symmetric after ligand titration, even at lowest drug concentration. The obtained values of T_m , ΔH_{cal} , van't Hoff enthalpy ΔH_v and the cooperativity η describing the ratio of calorimetric and van't Hoff enthalpy are listed in Table 2. ΔH_v was calculated from equation

$$\Delta H_v = \frac{4RT_m^2 C_p^m}{\Delta H_{cal}}$$

where R is gas constant.

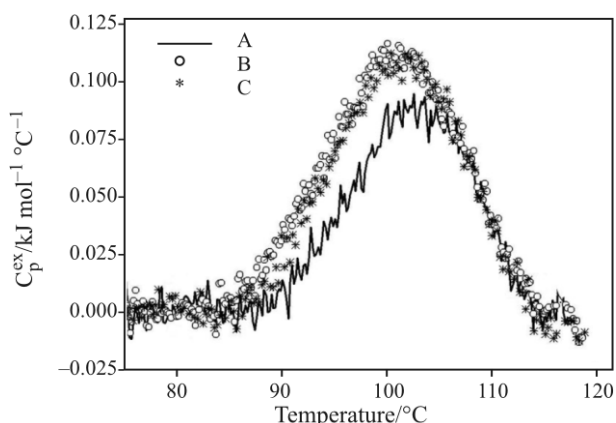
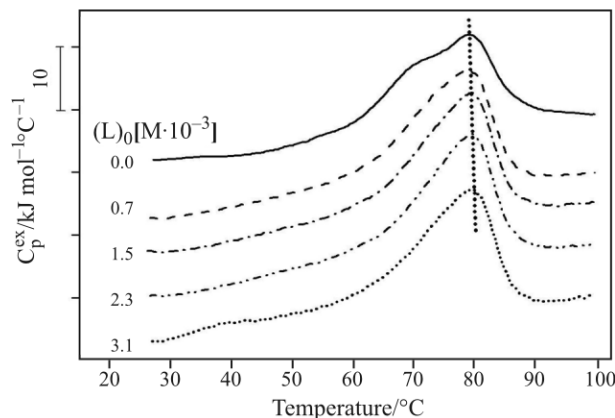

Fig. 2 DSC curves of ddi water solution stored for different times: A – fresh sample, B – after 6 h and C – after 12 h (scan rate 0.6 K min^{-1})

Fig. 3 DSC curves for thermal denaturation of HSA (0.015 mM) at different ddi concentration (scanning rate 1.0 K min^{-1})

Table 2 Thermodynamic parameters obtained from DSC scans ($\nu=1.0 \text{ K min}^{-1}$) of HSA (0.0155 mM) in the presence of ddi different concentration

[L/P]	$T_m/$ $^\circ\text{C}$	$\Delta H_{cal}/$ kJ mol^{-1}	$\Delta H_v/$ kJ mol^{-1}	η
0.0	78.6 ± 0.20	1192 ± 71	234 ± 16	5.1 ± 0.6
30.0	78.6 ± 0.04	1158 ± 54	255 ± 8	4.5 ± 0.3
50.0	79.0 ± 0.02	1129 ± 50	263 ± 4	4.3 ± 0.3
100.0	79.3 ± 0.03	1146 ± 37	284 ± 4	4.0 ± 0.1
151.0	79.5 ± 0.04	1092 ± 41	288 ± 12	3.7 ± 0.1
200.0	79.7 ± 0.03	1096 ± 83	280 ± 8	3.9 ± 0.4
302.0	79.9 ± 0.04	1112 ± 54	271 ± 8	4.0 ± 0.1
404.0	80.2 ± 0.03	1025 ± 87	305 ± 12	3.3 ± 0.1

T_m increases and ΔH_{cal} decreases with growth ddi concentration. Calculated values of η for HSA water solution indicate five cooperative units per mole of HSA what suggests that denaturation of HSA probably include five two-state transitions. ddi titration caused a little cooperativity drop. Observe changes in denaturation of HSA point out stabilizing role of ddi.

Kinetic analysis of thermal degradation of ddi water solution

Scan rate dependence and irreversibility of considered process suggest that the decomposition of ddi could be treated as kinetically controlled phenomenon. In this case the analysis of DSC data should begin with checking whether experimental data satisfy the one step model. Three criteria given in [9] were analyzed:

- $1/T$ vs. $\ln[\nu C_p^{ex}/(\Delta H_{cal} - \Delta H_T)]$, where ΔH_T is the heat evolved at given temperature T – plot should be approximated by straight line and the points corresponding to all the scanning rates should lie on a common straight line (Fig. 4a)

- $(1-\Delta H_T/\Delta H_{cal})^v$ vs. T – the points corresponding to all the scanning rates should lie on a common line (Fig. 4b)
- $\ln C_p^{ex}$ vs. $1/T$ – the identity of the curves shape obtained at various values of the scanning rates testifies to the validity of one-step irreversible model (Fig. 4c)

One can see from Fig. 4, that the results from DSC experiments met the requirements of foregoing criteria with small deviation. It follows that the degradation process of ddI water solution could be interpreted in terms of simple first-order one-step kinetic model.

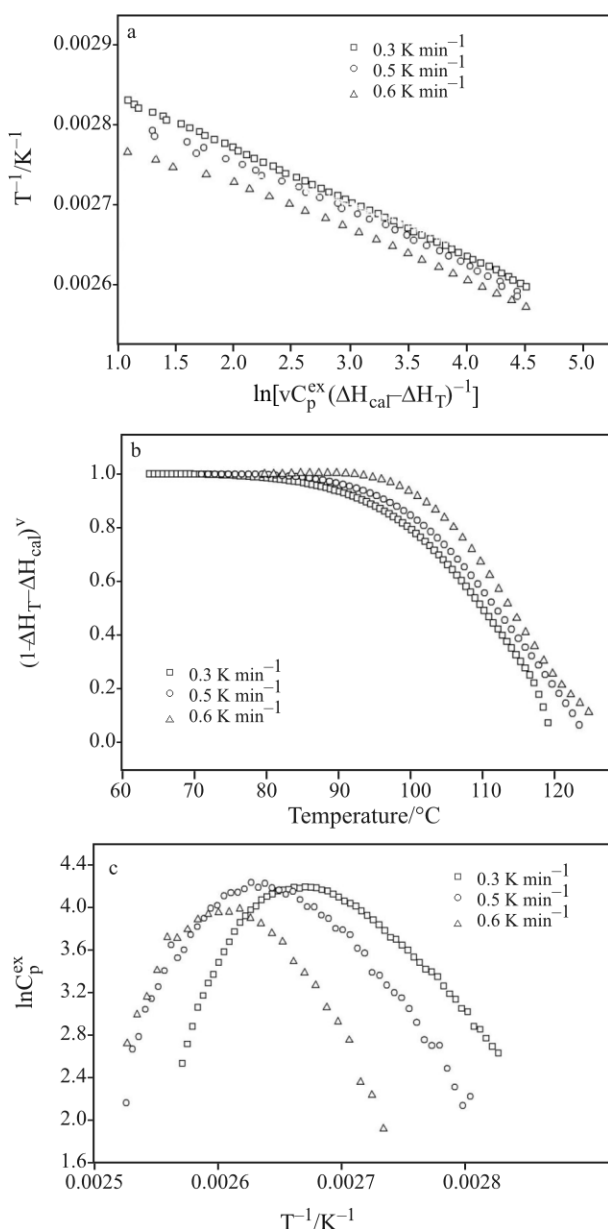


Fig. 4 The criteria for the one step irreversible model, dependence of a – $1/T$ on $\ln[vC_p^{ex}/(\Delta H_{cal}-\Delta H_T)]$, b – $(1-\Delta H_T/\Delta H_{cal})^v$ on T and c – $\ln C_p^{ex}$ on $1/T$ for ddI water solution

Another confirmation of one-step kinetic model validity is coincidence of activation energies E_A estimated in several different ways [10]:

- from the equation

$$k = vC_p^{ex} (\Delta H_{cal} - \Delta H_T)^{-1} \quad (1)$$

The energy of activation can be calculated from the slope of the Arrhenius plot, $\ln k$ vs. $1/T$.

- with using influence of v on T_m

$$\frac{v}{T_m^2} = \frac{AR}{E_A} e^{-E_A/RT_m} \quad (2)$$

a slope of the plot (v/T_m^2) vs. $1/T_m$ is equal $-E_A/R$

- from the dependence

$$\ln[\ln \Delta H_{cal} (\Delta H_{cal} - \Delta H_T)^{-1}] = \frac{E_a}{R} \left(\frac{1}{T_m} - \frac{1}{T} \right) \quad (3)$$

and a slope of the plot of $\ln[\ln \Delta H_{cal} (\Delta H_{cal} - \Delta H_T)^{-1}]$ vs. $1/T$ is equal $-E_A/R$ (Fig. 5).

- using the coordinates of the maximum of the calorimetric peak (T_m, C_p^m) according to:

$$E_a = 2.718RC_p^m T_m^2 \Delta H^{-1} \quad (4)$$

- The molar excess heat capacity function is given by [11]

$$\langle C_p(T) \rangle = \left(\frac{\Delta H_{cal} E_A}{RT_m^2} \right) \exp\left(\frac{E_A \Delta T}{RT_m^2} \right) \exp\left[-\exp\left(\frac{E_A \Delta T}{RT_m^2} \right) \right] \quad (5)$$

E_A values can be derived from non-linear least-squares fitting of Eq. (5) to the experimental data (Fig. 6).

Obtained values of E_A with use of 5 methods are listed in Table 3.

The differences in activation energy obtained for different scanning rates and using different methods are statistically essential what was verified by ANOVA test ($p < 0.02; 0.03$, respectively). According

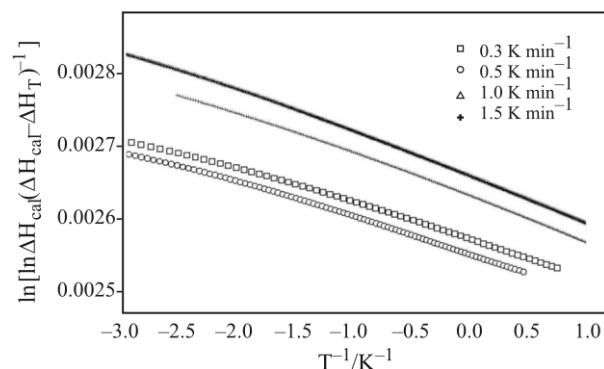
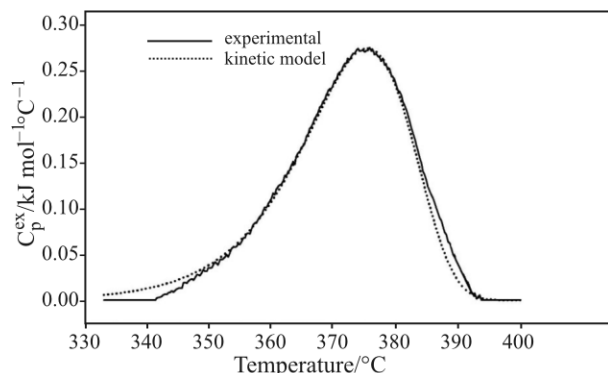


Fig. 5 Values of $\ln[\ln \Delta H_{cal} (\Delta H_{cal} - \Delta H_T)^{-1}]$ plotted for ddI (3.13 mM) vs. $1/T$ (method C)

Table 3 The activation energies E_A (kJ mol^{-1}) (\pm SEM) obtained for dDI water solution (3.13 mM) for different scanning rates ν (K min^{-1}) with use of five different methods A, B, C D and E

ν	A	B	C	D	E
0.3	140.3 \pm 12.8		143.1 \pm 15.4	139.6 \pm 12.0	138.5 \pm 11.4
0.5	131.2 \pm 14.4		144.7 \pm 5.9	134.1 \pm 5.6	135.2 \pm 7.9
0.6	146.5 \pm 2.4	124.5 \pm 19.3	159.2 \pm 3.0	154.5 \pm 0.7	140.2 \pm 4.8
1.0	143.7 \pm 7.0		157.8 \pm 14.3	158.2 \pm 12.0	131.5 \pm 10.2
1.5	149.6 \pm 3.3		169.1 \pm 1.9	130.8 \pm 8.5	145.3 \pm 10.4


Fig. 6 Fitting the experimental DSC profile by Eq. (5)

to the test Scheffe and Tukey the difference are statistically significant between scanning rate 30 and 40, 60 and 90 (in RIR Tukey=0.047, 0.01 and 0.046, respectively) and between methods B and C (in RIR Tukey=0.03).

Moreover Arrhenius plots (by Eq. (1)) allowed for calculating the rate constant k and half-life time $\tau_{1/2}$. Obtained plots (not shown) were extrapolated to lower temperatures in order to predict the values of k and $\tau_{1/2}$ at 25 and 37°C (Table 4).

Table 4 The rate constant k [h^{-1}] and half-life time $\tau_{1/2}$ [h] obtained in 25 and 37°C for dDI water solutions

$T/^\circ\text{C}$	$\tau_{1/2}/\text{h}$	$k \cdot 10^{-4}/\text{h}^{-1}$
20	53.3 \pm 8.2	2.1 \pm 0.9
25	22.7 \pm 5.5	5.6 \pm 1.4
30	8.7 \pm 1.0	13.1 \pm 2.5
37	2.7 \pm 0.5	43.2 \pm 9.2
40	1.6 \pm 0.3	71.6 \pm 11.1

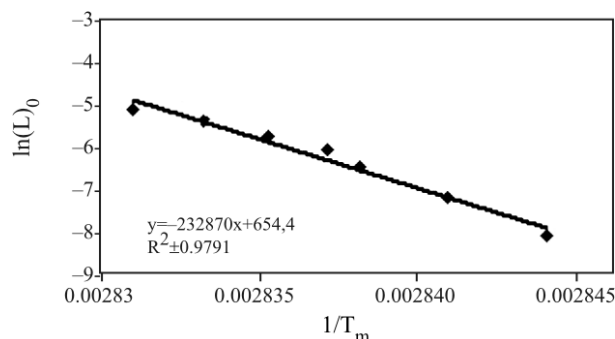
It should be noted that the temperature increase in the range from 20 to 25°C causes drop of $\tau_{1/2}$ value at about 30 h. One can conclude that the temperature influences markedly on dDI stability, so the carefullness in dDI storage should be kept.

Interaction of dDI with HSA

Relationship between ligand concentration L and denaturation temperature T_m in given concentration of protein is expressed by Eq. (6) [12]:

$$\frac{\Delta H_v}{RT_m} + n \ln(L)_0 = \frac{A}{n} + \left(\frac{\Delta C_p^0 T_m^0 - \Delta H_{\text{cal}}^0}{nR} \right) \frac{1}{T_m} + \frac{\Delta C_p^0 \ln(T_m/T_m^0)}{nR} \quad (6)$$

where T_m^0 , ΔH_{cal}^0 , and ΔC_p^0 are the temperature, enthalpy and heat capacity change for protein unfolding in the absence of ligand, n is the number of binding sites and $(L)_0$ is the total ligand concentration. The linear least square fit of Eq. (7) to the plot $\ln(L)_0$ vs. $1/T_m$ (Fig. 7) was done to obtain the number of binding sites n .


Fig. 7 The plot of $\ln(L)_0$ vs. $1/T_m$ for HSA in dDI presence

Then the binding constant K_L could be calculated from Eq. (7) [13]:

$$K_L(T_m) = \left[\exp \left[\frac{-\Delta H_{\text{cal}}}{R(1/T_m - 1/T_0)} + \frac{\Delta C_p}{R(\ln T_m/T_0 + T_0/T_m - 1)} \right] - 1 \right] [L]_{T_m} \quad (7)$$

where $[L]_{T_m}$ is the free ligand concentration $= (L)_0 - P_t/2$ and P_t is the total protein concentration.

Calculated values of $n=0.67 \pm 0.04$ and $K_L((4.0 \pm 0.8) \cdot 10^3 - (2.3 \pm 0.4) \cdot 10^3 \text{ mol}^{-1})$ in studied concentration range) indicate on weak HSA–dDI interaction. The analogous result $((9.7 \pm 1.5) \cdot 10^3 \text{ mol}^{-1})$ was also obtained for other nucleoside reverse transcriptase inhibitor–azidothymidine [14].

Conclusions

Thermal degradation of ddI in water solution is endothermic what was shown by the DSC study. Scan rate dependence and irreversibility indicate kinetically controlled process. Fulfillment of criteria given by Kurganov implies interpretation of ddI thermal degradation in terms of simple first-order one-step kinetic model. Calculated values of activation energies and half life times point at relatively small ddI stability what indicates better efficiency of fresh drug solutions.

Increase of transition temperature T_m for the human serum albumin in ddI presence suggests stabilizing role of this drug in HSA–ddI mixture. Obtained values of binding constant prove weak ddI affinity to the HSA molecule what is positive effect for the sake of drug bioavailability.

References

- 1 UNAIDS/WHO 2006 Report on the global AIDS epidemic.
- 2 C. Sánchez-Lafuente, S. Furlanetto, M. Fernández-Arévalo, J. Alvarez-Fuentes, A. M. Rabasco, M. T. Fauci, S. Pinzauti and P. Mura, *Int. J. Pharm.*, 237 (2002) 107.
- 3 X. Cahours, H. Dessans, P. Morin, M. Dreux and L. Agrofoglio, *J. Chrom. A*, 895 (2000) 101.
- 4 W. Zielenkiewicz, R. Swierzewski, F. Attanasio and G. Rialdi, *J. Therm. Anal. Cal.*, 83 (2006) 587.
- 5 G. Bruni, C. Milanese, G. Bellazzi, V. Berbenni, P. Cofrancesco, A. Marini and M. Villa, *J. Therm. Anal. Cal.*, 89 (2007) 761.
- 6 S. C. Mojumdar, M. Sain, R. C. Prasad, L. Sun and J. E. S. Venart, *J. Therm. Anal. Cal.*, 90 (2007) 653.
- 7 E. Lizarraga, C. Zabaleta and J. A. Palo, *J. Therm. Anal. Cal.*, 89 (2007) 783.
- 8 A. Schön, M. Del Mar Ingaramo and E. Freire, *Biophys. Chem.*, 105 (2003) 221.
- 9 B. I. Kurganov, A. E. Lyubarev, J. M. Sanchez-Ruiz and V. L. Shnyrov, *Biophys. Chem.*, 69 (1997) 125.
- 10 J. M. Sánchez-Ruiz, J. L. López-Lacomba, M. Cortijo and P. L. Mateo, *Biochemistry*, 27 (1998) 1648.
- 11 J. M. Sanchez-Ruiz, *Biophys. J.*, 61 (1992) 921.
- 12 M. S. Celej, S. A. Dassie, E. Freire, M. L. Bianconi and G. D. Fidelio, *Biochim. Biophys. Acta*, 1750 (2005) 122.
- 13 J. F. Brandts and L.-N. Lin, *Biochemistry*, 29 (1990) 6927.
- 14 A. Kluczewska, K. Michalik, Z. Drzazga and M. Kaszuba, *P. J. Env. Stud.*, 15/4A (2006) 59.

Received: September 27, 2007

Accepted: March 18, 2008

DOI: 10.1007/s10973-007-8795-z